pISSN 2384-1095
eISSN 2384-1109

iMRI 2021;25:300-312

https://doi.org/10.13104/imri.2021.25.4.300

iMRI
Investigative Magnetic Resonance Imaging

DEMO: Deep MR Parametric Mapping with Unsupervised Multi-Tasking Framework

Jing Cheng, Yuanyuan Liu, Yanjie Zhu, Dong Liang

Paul C. Lauterbur Research Center for Biomedical Imaging, Shenzhen Institutes of Advanced Technology, Chinese Academy of Sciences, Shenzhen, China

Compressed sensing (CS) has been investigated in magnetic resonance (MR) parametric mapping to reduce scan time. However, the relatively long reconstruction time restricts its widespread applications in the clinic. Recently, deep learning-based methods have shown great potential in accelerating reconstruction time and improving imaging quality in fast MR imaging, although their adaptation to parametric mapping is still in an early stage. In this paper, we proposed a novel deep learning-based framework DEMO for fast and robust MR parametric mapping. Different from current deep learning-based methods, DEMO trains the network in an unsupervised way, which is more practical given that it is difficult to acquire large fully sampled training data of parametric-weighted images. Specifically, a CS-based loss function is used in DEMO to avoid the necessity of using fully sampled k-space data as the label, thus making it an unsupervised learning approach. DEMO reconstructs parametric weighted images and generates a parametric map simultaneously by unrolling an interaction approach in conventional fast MR parametric mapping, which enables multi-tasking learning. Experimental results showed promising performance of the proposed DEMO framework in quantitative MR T1ρ mapping.

Keywords: Compressed sensing; Fast MR imaging; Parameter mapping; Unsupervised learning

Original Article

Received: June 7, 2021
Revised: September 5, 2021
Accepted: September 17, 2021

Correspondence to:
Dong Liang, Ph.D.
Paul C. Lauterbur Research Centre for Biomedical Imaging Institute of Biomedical and Health Engineering Shenzhen Institutes of Advanced Technology, Chinese Academy of Sciences Shenzhen, Guangdong, P. R. 518055, China.
Tel. +86-755-86392243
E-mail: dong.liang@siat.ac.cn

INTRODUCTION

Quantitative magnetic resonance (MR) parametric mapping is an emerging tool for the evaluation and determination of fundamental biologic properties of tissues. It aims to measure absolute MR relaxations, thus providing a comparable measurement across sites and time points (1, 2). The most common way to obtain an MR parametric map is by acquiring multiply parametric-weighted images with varying imaging parameters, e.g., inversion time (TI) in T1 mapping, echo time (TE) in T2 mapping, and spin-lock time (TSL) in T1ρ mapping. The parametric map is then estimated by fitting these images pixel by pixel with a corresponding physical exponential model. The scan time, proportional to the number of acquired images, is relatively long in MR parametric mapping, which greatly hinders its widespread use in clinical applications (3, 4).

Recently, some studies have tried to reduce the scan time of parametric mapping using compressed sensing (CS) (5-8) or low-rank matrix completion (LR) (9-11). These

methods can be classified into three categories based on their approaches. The first category follows the processing pipeline of conventional parametric mapping and only uses CS/LR to reconstruct parametric-weighted images. The second category uses models to directly reconstruct the parametric map from undersampled data without reconstructing numerous parametric-weighted images (12-16), thus avoiding error propagation in the fitting process. The third category uses an interaction approach. The prior information contained in the physical model is complemented with sparse or LR constraints in an interacting way, thus exhibiting superior performance to other methods (17-19). More details about these three categories of approaches can be found in a previous study (19). However, the reconstruction time of these CS/LR methods is very long. In addition, many parameters in the CS/LR model need to be tuned manually which are unacceptable in the clinic.

Deep learning recently has attracted a lot of interest in accelerating MR imaging (20-32). It can solve the above CS/LR issues by learning the nonlinear mapping function from input-output pairs in an end-to-end manner (20-26) or learning parameters, regularization function, even data consistency in an unrolling manner (27-32). Currently, there are only limited applications of deep learning for MR parametric mapping (33-35). For example, MANTIS (34) used a U-net mapping to generate a T_2 map from undersampled k-space data in an end-to-end manner. Cai et al. (33) applied an end-to-end ResNet to T_2 mapping from single-shot overlapping-echo detachment planar imaging. It can be seen that these existing methods all fill in the second category by using a deep network to directly reconstruct a parametric map from undersampled k-space data. Moreover, these methods are conducted in a supervised manner where the reference parameter map is given. However, supervised learning needs a large number of fully sampled k-space data which may be difficult to acquire in practice. In addition, reference parametric maps created by different fitting algorithms from fully sampled images might be slightly different. Therefore, unsupervised learning in fast MR parametric mapping is highly desired.

In this paper, we proposed a novel DEep MR parametric mapping method using unsupervised multi-tasking framewOrk (DEMO) to handle the situation where collecting a large number of fully sampled k-space data of the parametric-weighted images would be impractical. Specifically, a CS-based objective function including data consistency term and sparsity term was used as the loss function so that fully sampled k-space data or the reference parameter map would not be needed anymore. Besides, a multi-tasking learning strategy was developed to reconstruct parametric weighted images and generate a parametric map simultaneously. Moreover, the physics model was incorporated into the mapping task to enforce its output the same as the input in a self-supervised way. It could also interact with the reconstruction task. Therefore, DEMO is an interactive approach belonging to the third category. Comparisons were made with a sparsity-driven method rec-PF (36) and a low-rank and sparsity driven method k-t SLR (37) which also resorted solely to observed data. Experimental results using *in vivo* data sets showed that the proposed unsupervised framework achieved superior reconstruction and mapping performance.

A preliminary account of this work was previously presented as an abstract in ISMRM 2020 (38), where the CS objective function was used as the loss function to learn how to reconstruct a static image from its undersampled k-space data in a single task in an unsupervised manner. The performance of our proposed framework was demonstrated for T1ρ mapping of knee cartilage. However, it could also be applied to other quantitative MR parametric mapping using corresponding signal models.

METHODOLOGY

Fast MR Parametric Mapping

One of the important strategies to reduce MR parametric mapping scan time is to acquire k-space data with sub-Nyquist sampling. However, image reconstruction from undersampled k-space data is an ill-posed inverse problem. Directly reconstructing images from undersampled k-space data will result in aliasing artifacts in the image, which will then contaminate the parametric map. In such scenarios, additional prior information is often incorporated into the imaging model to facilitate the reconstruction. In the past decade, CS has attracted a lot of attention in accelerating MR imaging (39-41). It exploits the sparse prior of the image and solves the underlying constrained optimization problem to reconstruct images from highly undersampled k-space data. In general, the CS model for MR reconstruction can be formulated as a data consistency term and a sparse promoted term:

$$\min_{m} \; ||Am-f||_2^2 + \lambda||Dm||_1 \qquad [1]$$

where m is the image to be reconstructed, D is a sparse transform such as wavelet transform or total variation, A is the undersampled Fourier encoding matrix, f denotes the acquired k-space data, and λ is the regularization weight.

With well-reconstructed images, a parametric map can be generated using conventional fitting methods with an established physical model. Taking quantitative $T_{1\rho}$ mapping as an example, $T_{1\rho}$-weighted images follow an exponential decay as follows:

$$M = S(M_0, T_{1\rho}) = M_0 \exp(-TSL_k/T_{1\rho})_{k=1,2,\ldots,N} \quad [2]$$

where M is the image obtained at varying TSLs and M_0 is the equilibrium image obtained without applying a spin-lock pulse (called "baseline image" hereafter). Once $T_{1\rho}$-weighted images are obtained, $T_{1\rho}$ map can be generated linearly by fitting along the TSL direction pixel by pixel following model [2], which can be linearized by applying the logarithm to both sides.

However, the prior information of the signal relaxometry model is not fully utilized in such a two-step manner to generate a parametric map from undersampled k-space data. To better explore the prior provided by the signal model, the predictability of the parametric model can be introduced into the parametric weighted image reconstruction. Figure 1 illustrates a flowchart of this interaction approach of the third category. The prior information contained in the parameter model could increase data redundancy within parametric weighted images so that performances of both image reconstruction and parametric map fitting could be improved (17-19).

Deep MR Imaging

Although CS-based reconstruction methods can achieve high performance with many theoretical guarantees, the sparsity prior is usually enforced by fixed sparsifying transforms or linear dictionaries, which can restrict the performance of CS in pursuing higher acceleration factors. The deep learning approach goes beyond CS by exploiting the image prior through network learning from large training data. It can be approximately categorized into two types: those based on unrolled algorithms and those not based on unrolled algorithms (42). With the unrolling-based approach, an iterative algorithm used for solving an inverse problem is unrolled to a deep network in which all free parameters and functions can be learned through network training. For the approach that is not based on unrolling, it employs an end-to-end network to learn the mapping between the network input and output. In the current field of deep MR parametric mapping, an end-to-end network is usually selected to generate a parametric map in a supervised manner.

Overview of DEMO

In supervised learning for image reconstruction, parameters of the network update through training to achieve the lowest error between the network output and the ground truth, which is usually controlled by the loss function of mean square errors (MSE). Since there are no fully sampled k-space data to produce training pairs, it

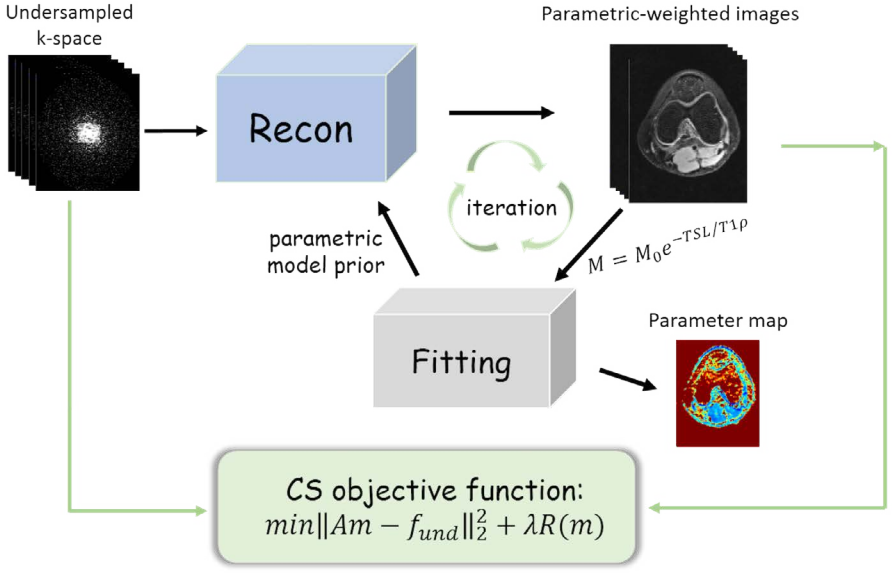

Fig. 1. Schematic illustration of the interaction approach in fast MR parameter mapping. Parameter-weighted images and the corresponding parameter map are iteratively updating through an optimization algorithm that minimizes the CS objective function, where (m) denotes the sparse prior.

is necessary to find an alternative loss function without labels involved. CS searches the solution that minimizes the objective function [1]. Deep learning aims to train the network that could minimize the loss function which induces the training direction of the network. It comes naturally that the objective function of CS [1] can be used as the loss function of deep networks in that the network searches the optimal one among all potential solutions given partial sampled data and sparse constraints. In such scenarios, no ground-truth or fully sampled data are needed. Inspired by this idea and given the fact that the parameter map is usually estimated from parameter-weighted images, DEMO adopts the CS objective function [1] as the loss function in network training. Specifically, the loss function used for network training in DEMO was defined as follows:

$$L(\Theta) = \frac{1}{N}\sum_{j=1}^{N} || AM(\Theta,f)-f^{k} ||_2^2 + \lambda || M(\Theta,f) ||_{TV} \quad [3]$$

where $M(\Theta, f)$ was the parametric-weighted images based on network parameter Θ and undersampled k-space data f, and $|| \cdot ||_{TV}$ was the total variation (TV) regularization.

In conventional fast MR parametric mapping, the third category of approach involves parametric map updating during iterations of reconstruction. This scheme enables better performance than the first category of approach which isolates steps of image reconstruction and parameter map fitting. DEMO unrolls this iteration as a deep network with a reconstruction module and a fitting module as shown in Figure 1. All these are implemented using deep learning. Specifically, a deep learning-based parameter map fitting interacted with deep unrolled reconstruction to improve both reconstruction quality and parameter mapping. The whole procedure can be formulated as follows:

$$\begin{cases} m_{n+1} = \Gamma(Am_n, A\tilde{m}_n, f) \\ (M_0, T_{1\rho})_{n+1} = U(m_{n+1}) \\ \tilde{m}_{n+1} = S(M_0, T_{1\rho})_{n+1} \end{cases} \quad [4]$$

where n is the iteration number, m is the parametric-weighted image (here refers to T1ρ-weighted image from deep unrolling reconstruction Γ), $(M_0, T_{1\rho})$ is the baseline image and associated $T_{1\rho}$ map which are generated simultaneously from network U, $\tilde{m}$ is the synthetic $T_{1\rho}$ -weighted images satisfying the $T_{1\rho}$ signal decay as in model [2].

Figure 2 presents an overview of the proposed framework DEMO. There are two chained networks in the framework that generate reconstructed images and $T_{1\rho}$ map directly from undersampled k-space data. One sub-network named Recon-net is used for image reconstruction and the other Mapping-net is used to estimate $T_{1\rho}$ map and baseline image M_0 with input images from Recon-net. A physical model was incorporated after Mapping-net to generate T1ρ -weighted images, which were then used as inputs of the next Recon-net.

Details of each sub-network are as follows:

1) Recon-net: The network used for reconstruction is the modified PD-net, which is the unrolling version of the primal-dual algorithm. It has been applied to accelerate MR imaging successfully (43). In Recon-net, the formulation can be written as follows:

$$\begin{cases} d_{n+1} = \Gamma(d_n, Am_n, A\tilde{m}_n, f) \\ m_{n+1} = \Lambda(m_n, \tilde{m}_n, A^* d_{n+1}) \end{cases} \quad [5]$$

where d is the dual variable. Figure 3a illustrates one

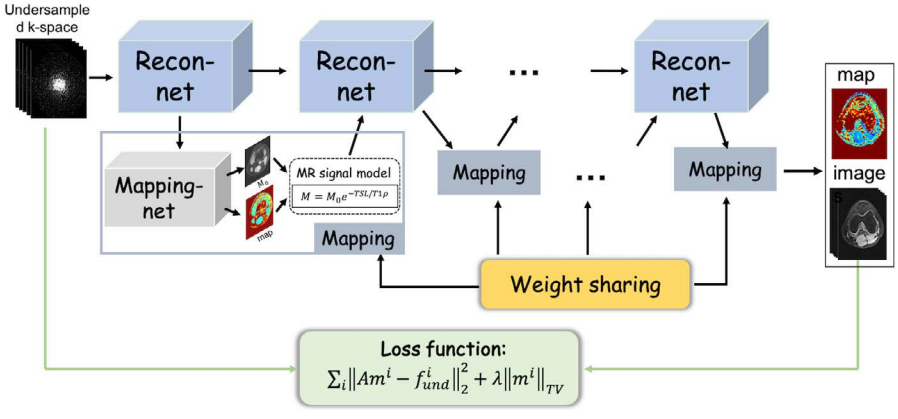

Fig. 2. Overview of the proposed framework DEMO. The CS-based loss function make DEMO an unsupervised framework, and the two chained sub-networks Recon-net and Mapping-net complete the tasks of images reconstruction and parametric map estimation, respectively. The physical model is used to connecting the two tasks.

iteration block of Recon-net. The dual block Γ accepts four 4D tensors input and performs three layers of 2D convolution with filter size 3 × 3. The two channels of input tensors represent real and imaginary parts of complex-valued MR data. The number of feature maps is denoted on the top of each layer. To train the network more easily, we made it a residual network. The iteration number was set to be 5.

2) Mapping-net: A modified U-net used for generating (M_0, $T_{1\rho}$) is described in Figure 3b. Several modifications were made to accommodate the proposed framework. First, a convolutional layer with stride 2 was used to down-sample the image instead of using the max-pooling layer to make the network a fully convolutional network. Second, the left side feature was directly added to the right side instead of concatenation operations to reduce the number of training parameters. Third, Bi-linear interpolation was used for the up-sampling layer to reduce checkerboard artifact. Fourth, since the image was complex-valued and the parameter map was always non-negative, the out channel of the M_0 generating branch was 2 representing real and image parts of M_0. The last layer of the map generating branch was the 2D convolution followed by a ReLU activation. The out channel was 1. The last layer in the two branches uses a kernel of size 1 × 1. Weights of Mapping-net were shared across iterations to reduce the number of training parameters.

EXPERIMENTAL RESULTS

Datasets

Six healthy volunteers (2 males aged 26 ± 2 years old and 4 females aged 45 ± 15 years old) were recruited for $T_{1\rho}$ scanning. Informed consent was obtained from the imaging object in compliance with the IRB policy. All MR scans were performed with a 3T scanner (uMR 790, United Imaging Healthcare, Shanghai, China) using a commercial 12-channel phased-array knee coil. $T_{1\rho}$-weighted images of the knee were acquired using a 3D modulated flip angle technique in refocused imaging with an extended echo train (MATRIX) sequence and a self-compensated paired spin-lock preparation pulse. The spin-lock frequency was fixed at 500 Hz (equivalent to a spin-lock pulse field strength of 11.74 μT). Imaging parameters were as follows: TE/TR = 8.96/2000 ms, echo train length = 60, FOV = 250 × 143 × 143, matrix size = 256 × 146 × 124, recon pixel size = 0.98 × 0.98 ×0.98 mm^3, echo spacing = 4.48 ms, and TSLs = 5, 10, 20, 40, and 60 ms. The total scan time for the fully sampled k-space data with elliptical scanning was 39 minutes and 30 seconds, which would be unacceptable in the clinic. Fully sampled multi-coil k-space data were adaptively combined to single-coil data (44) and then cropped to 256 × 144 × 124 to be treated as references only for evaluating performance in the comparison. These fully sampled data were then retrospectively undersampled using Poisson-disk

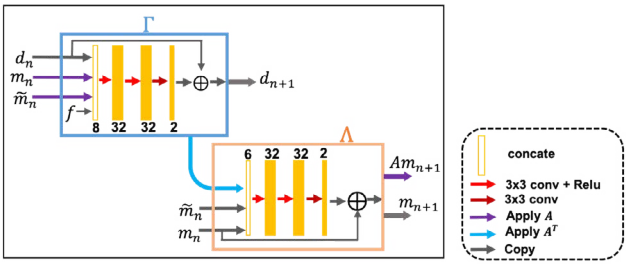

a

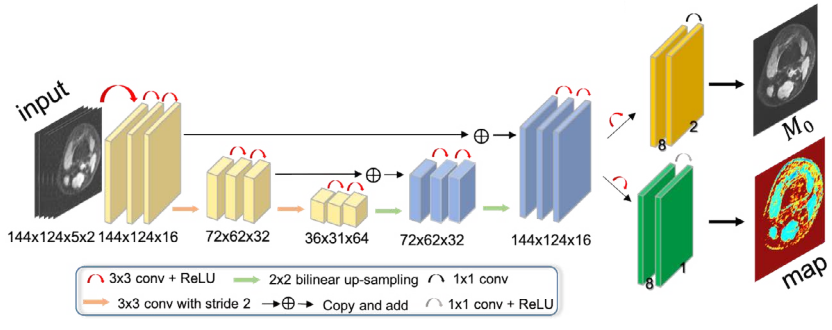

b

Fig. 3. Architectures of the networks used in DEMO. (a) The n-th iteration block in Recon-net. Both dual iteration Γ and primal iteration Λ adopt a 3-layer CNN and residual learning. (b) The Mapping-net. A modified U-net architecture is used to generate a parametric map.

random patterns with net accelerations of 5.2 and 7.6 to generate undersampled data. Noted that the sampling mask at each TSL had the same acceleration factor but different sampling locations.

Network Training

Undersampled data were concatenated together from all five TSLs with two channels representing real and imaginary parts. Thus, the input of Mapping-net had a total of 10 channels. In Recon-net, the dimension of these five TSLs was embedded in the batch dimension due to the 2D convolution used. Of the six subjects, four (generating 780 selected 3D training data) were used for training and the remaining two subjects were used for testing. Of a total of 780 slices in the training union, 700 slices were randomly selected for training the network.

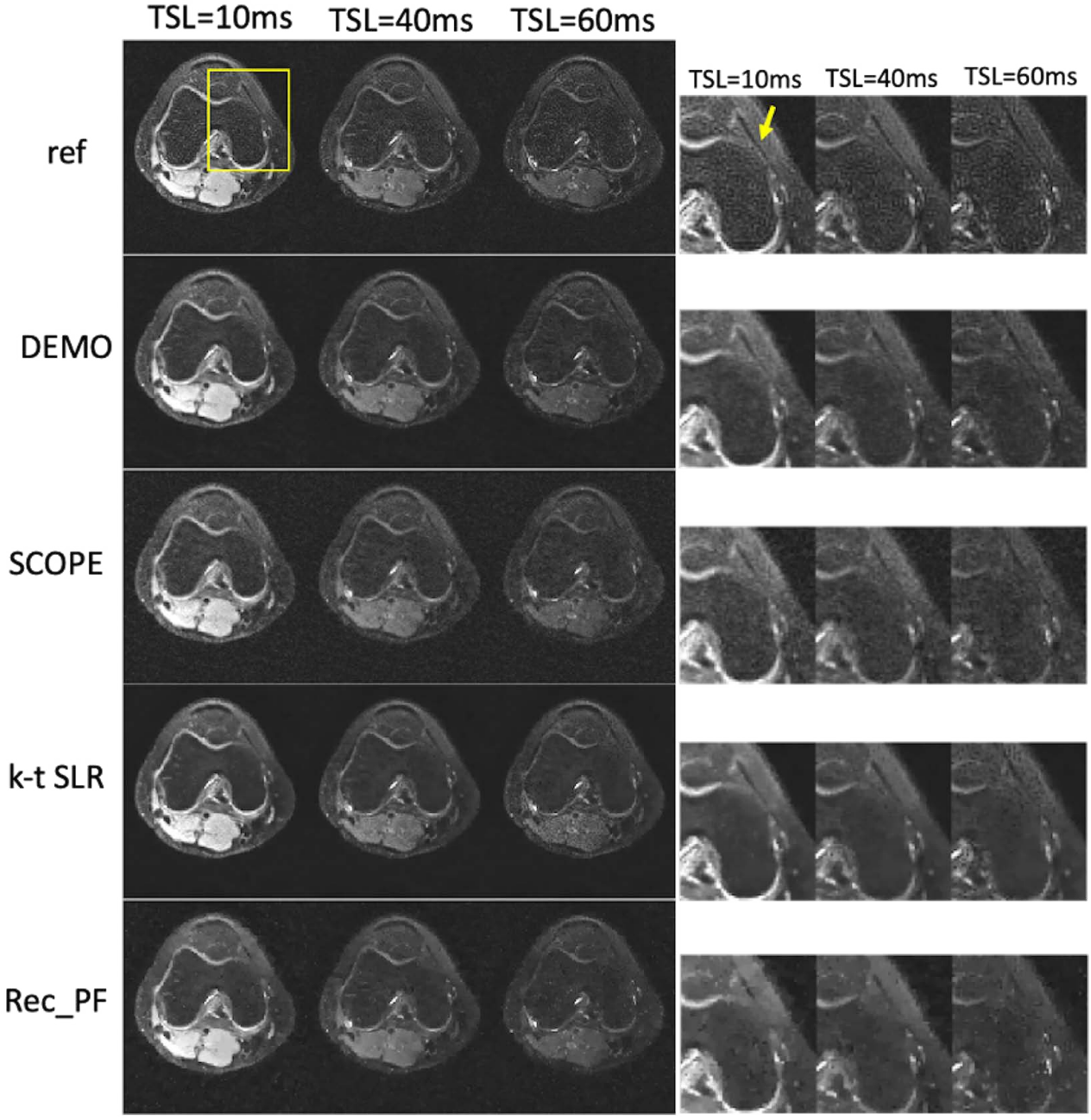

Fig. 4. Reconstruction images at three TSLs from an axial view with an acceleration factor of 5.2 from subject 1. Zoom-in images of the enclosed part are provided in the right column to give detail comparisons.

The input of the framework included undersampled k-space data and sampling mask. The output of the framework was the $T_{1\rho}$ map, the baseline image M_0, and the weighted image generated by (M_0, $T_{1\rho}$). The generated weighted image was then used for calculating CS-based loss [3]. The network was trained in a minibatch manner with 10 image slices in a single minibatch. ADAM optimizer was used to update network weights. The learning rate followed an exponential decay with an initial value of 0.001 and a decay rate of 0.95. The parameter in the loss function [3] was empirically selected as $\lambda = 0.0003$. To investigate the influence of different weighting parameter, additional experiments were conducted with $\lambda = 0.0001$, $\lambda = 0.0005$, and $\lambda = 0.001$.

The entire framework was implemented on an Ubuntu 16.04 LTS (64-bit) operating system equipped with a Tesla TITANXp Graphics Processing Unit (GPU, 12GB memory) in the open framework Tensorflow with CUDA and CUDNN support. The network training took approximately 1 hour with 200 epochs.

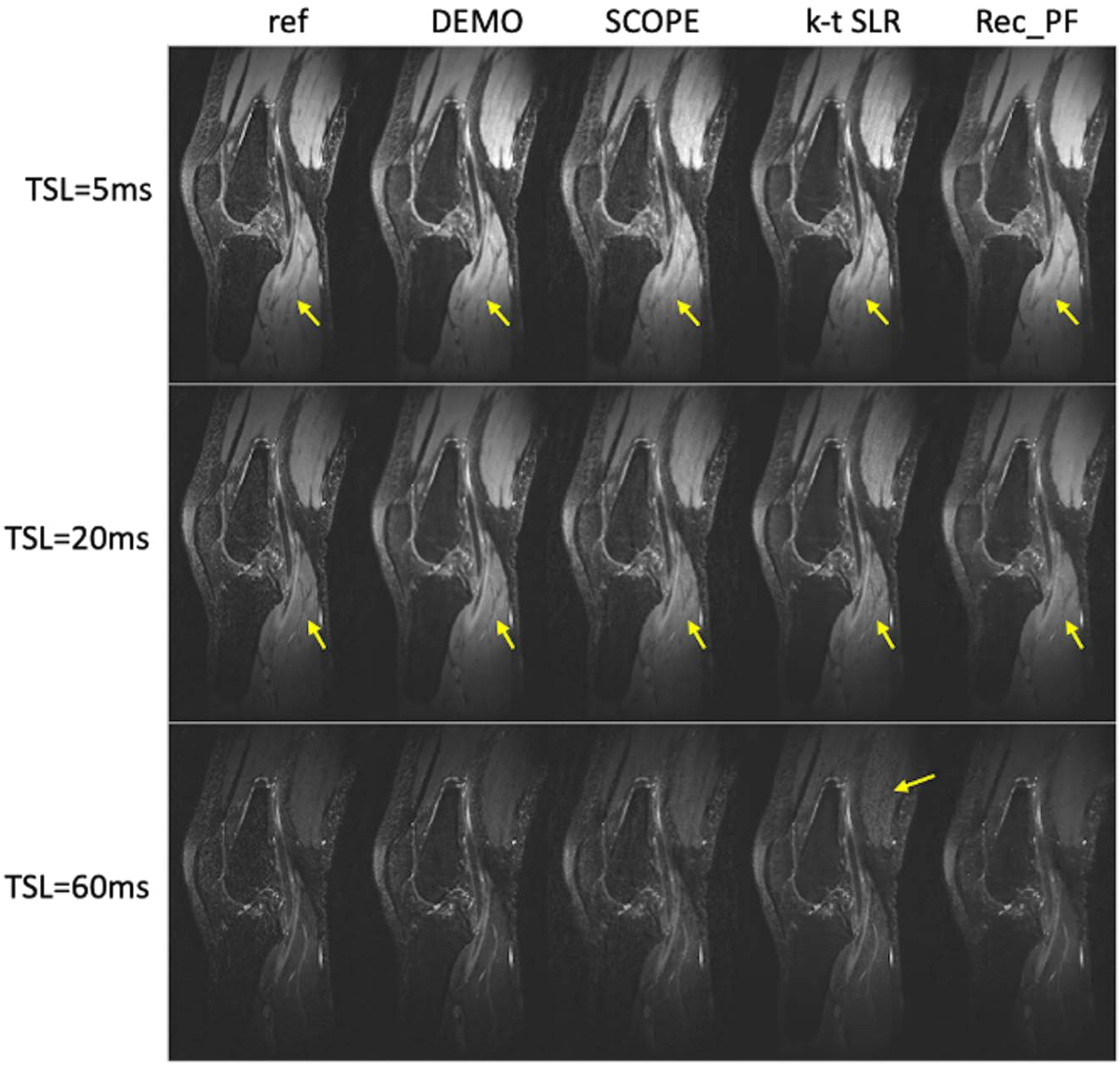

Fig. 5. Comparison of reconstructed images with different reconstruction methods at three TSLs with R = 5.2 from the other subject. The proposed DEMO showed better performance in detail preservation and noise suppression indicated by arrows.

Evaluation

The performance of the proposed framework DEMO was evaluated by comparing with ① conventional sparsity-based reconstruction approaches using a TV regularization (Rec_PF), a combination of low-rank and sparsity constraint (k-t SLR) on the multi-TSL image series (both belonging to the first category that only reconstructs the parametric-weighted images and then estimates the parametric map), and the parametric signal compensation method (SCOPE) (belonging to the third category that the parametric map estimation is interacted in the pipeline of reconstruction); ② direct CNN training which used only "Mapping-net" mentioned above to generate a parametric map from undersampled multi-TSL images (referred to as "Mapping-net" hereafter, which belongs to the second category that estimates the parametric map directly from raw data); and ③ a 2-step CNN approach which used the Recon-net mentioned above to reconstruct the multi-TSL image series and then used the fitting algorithm [2] to fit the parametric map (referred as "Recon-net + Fitting", belonging to the first category).

$T_{1\rho}$ map of the region-of-interest (ROI) was overlaid on the reconstructed $T_{1\rho}$-weighted image at TSL= 5 ms to compare mean values and standard deviations of $T_{1\rho}$ in cartilage from rec-PF, k-t SLR, SCOPE, Mapping-net, Recon-net + Fitting, and the proposed DEMO at R = 5.2 with reference T1ρ values from fully sampled images.

RESULTS

Figure 4 shows reconstruction results of $T_{1\rho}$-weighted images from different reconstruction methods at R = 5.2 for subject 1. Images reconstructed with rec-PF showed apparent detail loss and noticeable artifacts. Although k-t SLR reconstruction demonstrated improved image quality than rec-PF, it still showed signal loss and noise, especially at long TSLs. SCOPE did not perform well for the balance of artifact removal and detail preservation. However, the proposed DEMO generated nearly artifact-free reconstructions with well-preserved features.

Sagittal views of reconstructed images are shown in Figure 5. With short TSLs (5 ms and 20 ms), DEMO had a better depiction of fine details. It also showed better performance for noise suppression, consistent with the axial view shown in Figure 4. Although Rec_PF did better for artifact removing, it was too smooth in the image that useful features might last.

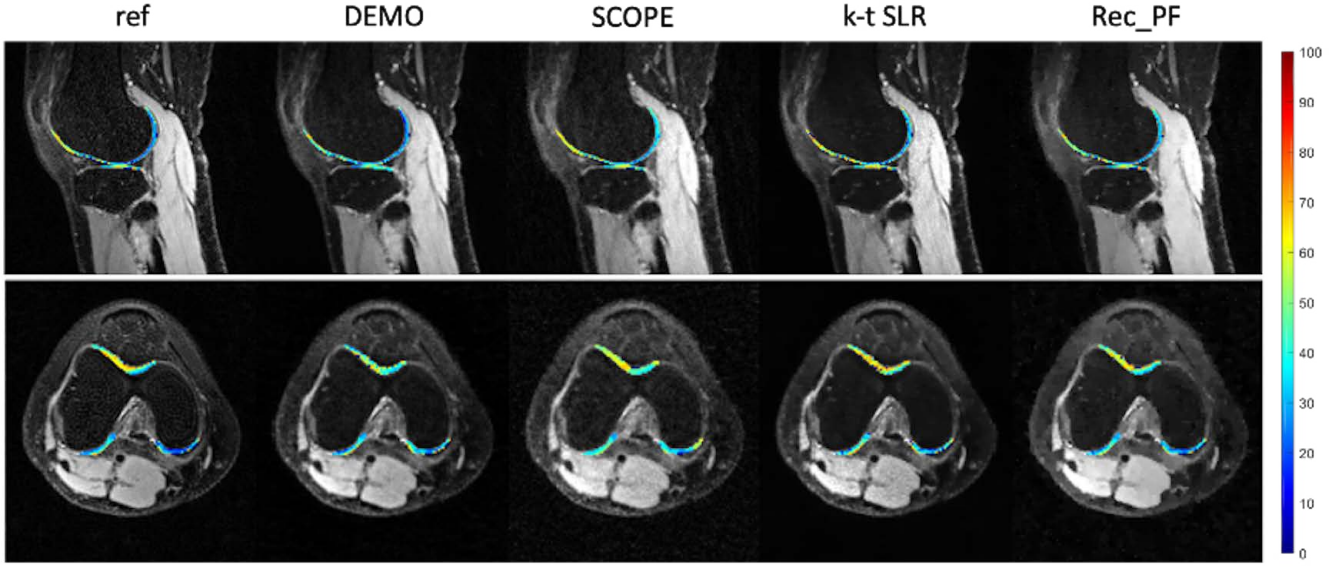

35.1287 (2.8558)	**35.9022** (2.7297)	39.5442(3.0028)	40.2087 (3.2316)	38.4726 (3.0174)
42.1005 (4.6503)	**42.5757** (4.6446)	44.2786(4.8296)	49.9515 (5.3895)	43.6766 (4.6920)

Fig. 6. Estimated $T_{1\rho}$ parameter maps for selected cartilage ROIs with sagittal and axial views overlaid on reconstructed $T_{1\rho}$ -weighted images at TSL = 5 ms for R = 5.2 from subject 1. The reference image and corresponding $T_{1\rho}$ parameter maps were obtained from fully sampled k-space data. Mean values and standard deviations of ROI $T_{1\rho}$ maps are also provided.

Figure 6 shows sagittal and axial views of the same dataset used for Figure 4 at TSL = 5ms. Selected ROIs of $T_{1\rho}$ map were overlaid on reconstructions. ROI $T_{1\rho}$ mean values and standard deviations of different methods are also provided. DEMO gave the most similar values of $T_{1\rho}$ to the reference with the lowest standard deviation.

Although displayed images reconstructed from k-t SLR showed better quality than those from Rec_PF, the parametric map was not. This was because reconstructed images showed severer noise at long TSLs from k-t SLR (seen in Figs. 4, 5), which might have a deleterious effect on parameter estimation. SCOPE did a better job than k-t SLR due to interactions between the parametric-weighted image reconstruction and map estimation.

To test the stability of DEMO, the network trained with a specific sampling ratio was evaluated using data with other sampling ratios. As shown in Figure 7, data with R = 7.2 could be well reconstructed from the network trained with R = 5.2, demonstrating the flexibility of DEMO for changing acceleration factors. Although there was a little over smoothing in the reconstructed image with R = 7.2, the bias of $T_{1\rho}$ values was still acceptable considering that fewer data were acquired.

Figure 8 shows results of reconstructions using different deep learning methods at R = 5.2 for subject 1. Images reconstructed with Mapping-net and Recon-net separately were over-smoothed (indicated by yellow arrows in the image) than those with DEMO.

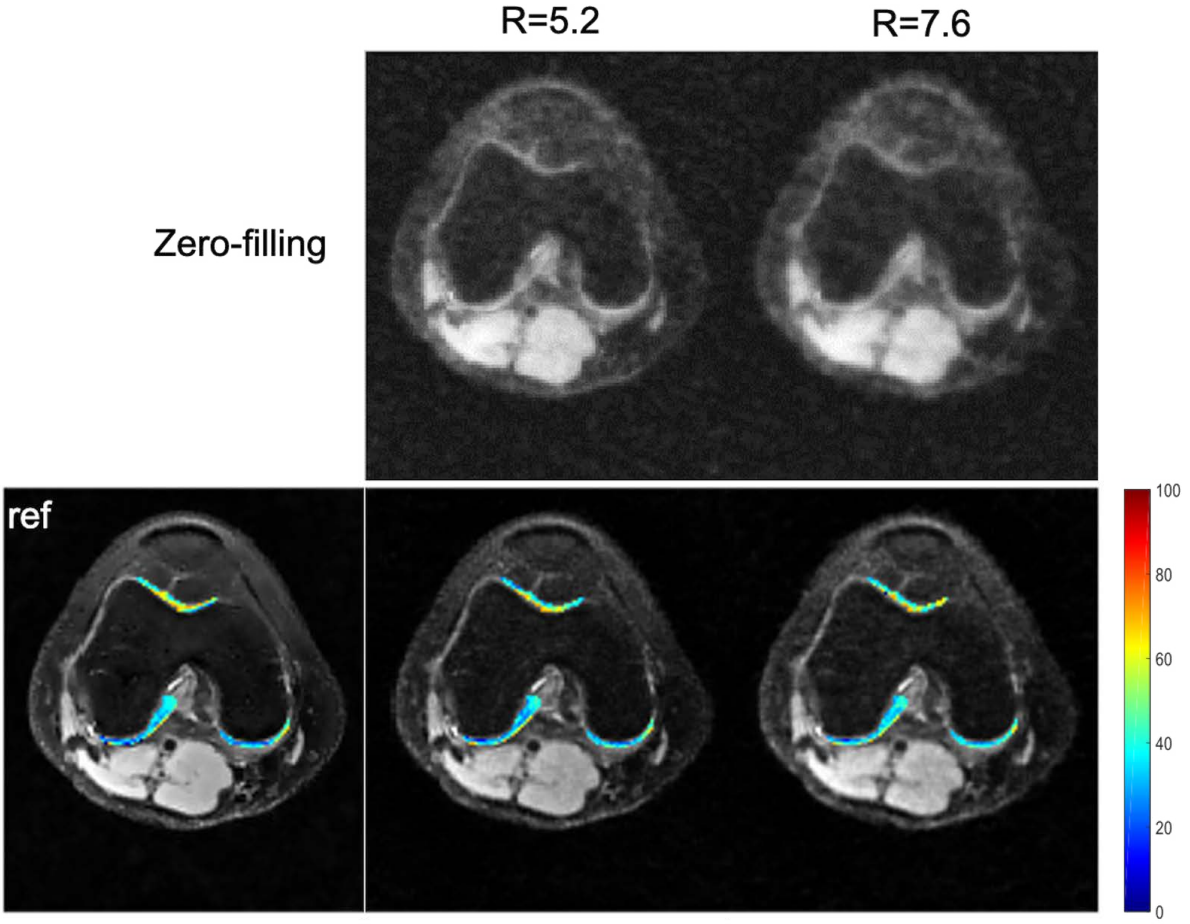

mean	39.3285	39.2043	40.3455
std	4.5431	4.5216	4.5832

Fig. 7. Estimated $T_{1\rho}$ parameter maps from DEMO for selected cartilage ROIs with axial view overlaid on reconstructed $T_{1\rho}$ -weighted images at TSL = 5 ms for different acceleration factors from subject 1 (second row). Corresponding zero-filling images are also provided (first row).

DEMO showed a similar performance to reference in $T_{1\rho}$ estimation, while Recon-net + Fitting performed worse, showing approximately 3 ms of bias compared to reference in mean value of ROI. Mapping-net showed worse performance than the other two deep learning-based methods. The main reason why DEMO performed better than Recon-net + Fitting and Mapping-net was due to the interaction strategy that the physical model prior could improve parametric-weighted image reconstruction and that better reconstructed parametric-weighted images could improve the parametric map estimation. Nevertheless, the method of Mapping-net took the shortest time to generate a parametric map as it only needed to perform one forward process of a U-net. Recon-net + Fitting took the longest time due to the conventional fitting algorithm [2] known to fit the parametric map pixel by pixel. DEMO generated the parametric map in a reasonable time as its reconstruction and the map estimation were both accomplished by networks.

Figure 9 illustrates the performance of DEMO with different λ values in loss function at R = 5.2. The reconstruction quality is affected by the weighting parameter. Just as in conventional CS optimization, a large regularization parameter (λ = 0.001) will result in over-smooth in the image while a small parameter (λ = 0.0001) will show artifacts. With an appropriate parameter (λ = 0.0003), the reconstruction showed good artifact suppression and detail preservation. There were few differences among $T_{1\rho}$ maps with a broad range of regularization parameters.

CONCLUSION AND OUTLOOK

In this paper, an unsupervised deep learning framework called DEMO was proposed for accelerating MR parametric mapping. The core novelty of DEMO is that it uses a CS-based loss function to train the network without needing fully sampled training data. The entire reconstruction framework can be formulated as an unrolled version of the interaction approach, which alternatively updates parametric-weighted images reconstruction and parameter map estimation. This alternative updating strategy allows DEMO to accomplish both image reconstruction and map fitting tasks with improved performance for each task due to interactions between them.

The unsupervised training strategy used in DEMO can be applied to other supervised networks by replacing the loss function with the corresponding CS objective function in the case where fully sampled k-space data are not acquired.

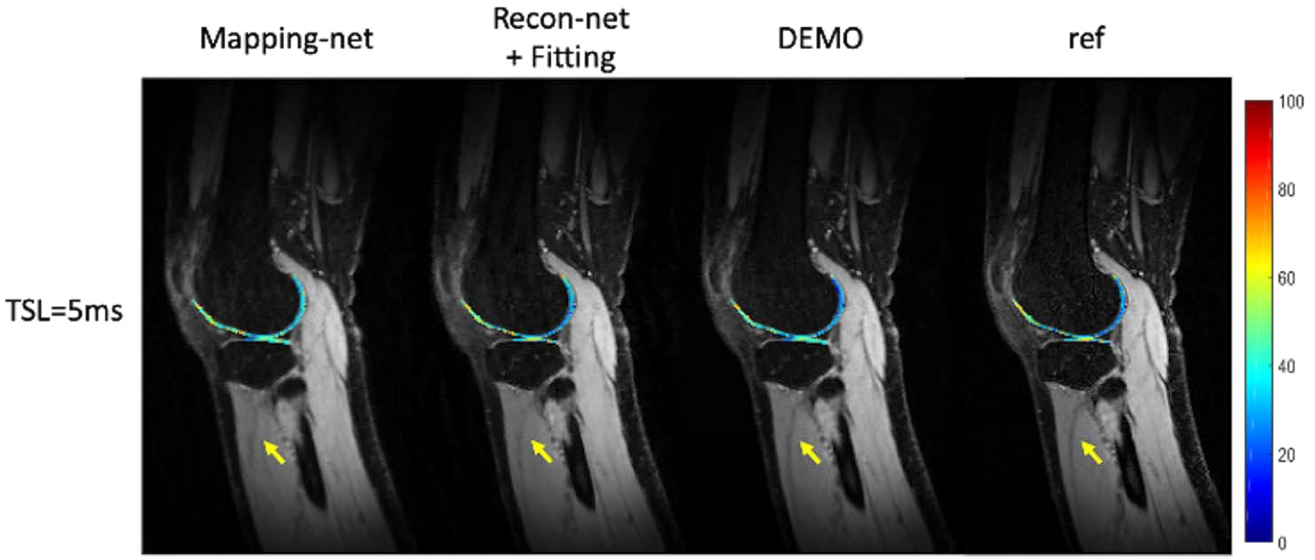

	Mapping-net	Recon-net + Fitting	DEMO	ref
mean	41.4163	38.7130	35.9022	35.1287
std	3.0684	2.9464	2.7297	2.8558

Fig. 8. Comparison of reconstructed images and $T_{1\rho}$ map for selected cartilage ROIs using DEMO with images and $T_{1\rho}$ map generated using Mapping-net and Recon-net + Fitting at R = 5.2.

Therefore, it can be easily extended to other applications, such as conventional static imaging and dynamic imaging. Our preliminary work showed that this strategy achieved better performance than CS in reconstructing static images. Moreover, it provides an alternative way to solve a CS optimization problem besides the traditional iterative reconstruction method and the deep-learning unrolling method.

Although the feasibility of DEMO was evaluated for accelerating mono-exponential $T_{1\rho}$ mapping of the knee in this study, this framework could be extended to more advanced signal models such as the multi-exponential model (45-47).

Our study has several limitations. All experiments were performed using single-coil data. Although the proposed method achieved a high acceleration factor of 7.6, multi-coil data containing coil sensitivity information and more data redundancy might further improve the reconstruction accuracy and acceleration factor. The network performance using multi-coil data will be explored in our further work. Another improvable aspect was the selection of regularization parameter in our loss function. Automatically choosing optimized regularization parameter in an adversary manner might be a more stable and flexible approach to solve this issue.

Acknowledgments

This work was supported partly by the National Natural Science Foundation of China (61771463, 81830056, U1805261, 81971611, 61871373, 81729003, 81901736), National Key R&D Program of China (2017YFC0108802 and 2017YFC0112903), Natural Science Foundation of Guangdong Province (2018A0303130132), Shenzhen Peacock Plan Team Program (KQTD20180413181834876), Innovation and Technology Commission of the government of Hong Kong SAR (MRP/001/18X), Strategic Priority Research Program of Chinese Academy of Sciences (XDB25000000), China Postdoctoral Science Foundation

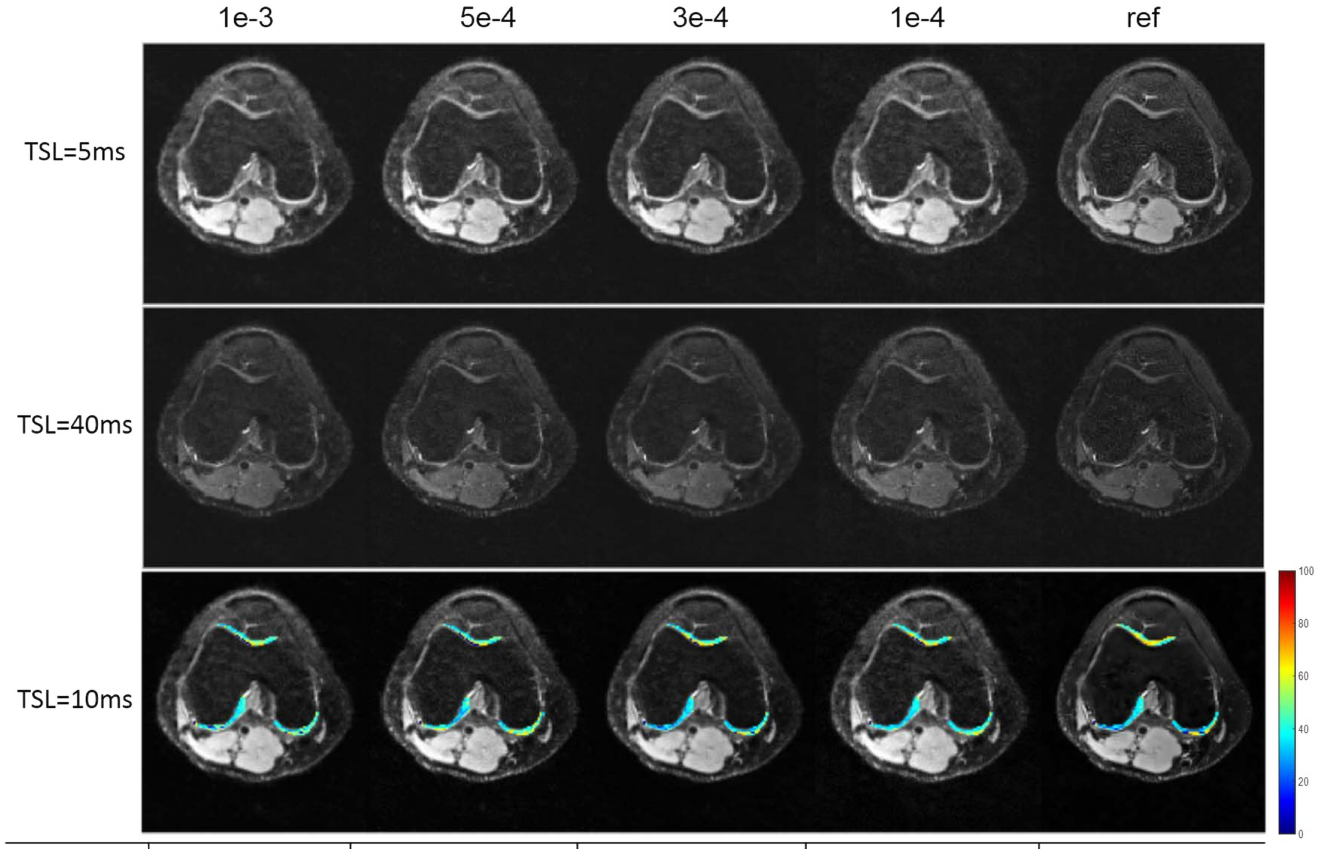

mean	40.9825	42.1040	42.1611	43.7114	42.6576
std	5.1710	5.3812	5.1983	5.2613	5.4987

Fig. 9. Comparison of reconstructed images and $T_{1\rho}$ map for selected cartilage ROIs using DEMO with different λ at R = 5.2.

(2021M693316), and SIAT Innovation Program for Excellent Young Researchers (E1G031).

REFERENCES

1. MacKay A, Whittall K, Adler J, Li D, Paty D, Graeb D. In vivo visualization of myelin water in brain by magnetic resonance. Magn Reson Med 1994;31:673-677
2. Sibley CT, Noureldin RA, Gai N, et al. T1 Mapping in cardiomyopathy at cardiac MR: comparison with endomyocardial biopsy. Radiology 2012;265:724-732
3. Duvvuri U, Charagundla SR, Kudchodkar SB, et al. Human knee: in vivo T1(rho)-weighted MR imaging at 1.5 T--preliminary experience. Radiology 2001;220:822-826
4. Regatte RR, Akella SV, Lonner JH, Kneeland JB, Reddy R. T1rho relaxation mapping in human osteoarthritis (OA) cartilage: comparison of T1rho with T2. J Magn Reson Imaging 2006;23:547-553
5. Petzschner FH, Ponce IP, Blaimer M, Jakob PM, Breuer FA. Fast MR parameter mapping using k-t principal component analysis. Magn Reson Med 2011;66:706-716
6. Velikina JV, Alexander AL, Samsonov A. Accelerating MR parameter mapping using sparsity-promoting regularization in parametric dimension. Magn Reson Med 2013;70:1263-1273
7. Zhou Y, Pandit P, Pedoia V, et al. Accelerating T1rho cartilage imaging using compressed sensing with iterative locally adapted support detection and JSENSE. Magn Reson Med 2016;75:1617-1629
8. Pandit P, Rivoire J, King K, Li X. Accelerated T1rho acquisition for knee cartilage quantification using compressed sensing and data-driven parallel imaging: a feasibility study. Magn Reson Med 2016;75:1256-1261
9. Pedersen H, Kozerke S, Ringgaard S, Nehrke K, Kim WY. k-t PCA: temporally constrained k-t BLAST reconstruction using principal component analysis. Magn Reson Med 2009;62:706-716
10. Zhang T, Pauly JM, Levesque IR. Accelerating parameter mapping with a locally low rank constraint. Magn Reson Med 2015;73:655-661
11. Zhao B, Lu W, Hitchens TK, Lam F, Ho C, Liang ZP. Accelerated MR parameter mapping with low-rank and sparsity constraints. Magn Reson Med 2015;74:489-498
12. Block KT, Uecker M, Frahm J. Model-based iterative reconstruction for radial fast spin-echo MRI. IEEE Trans Med Imaging 2009;28:1759-1769
13. Sumpf TJ, Uecker M, Boretius S, Frahm J. Model-based nonlinear inverse reconstruction for T2 mapping using highly undersampled spin-echo MRI. J Magn Reson Imaging 2011;34:420-428
14. Welsh CL, Dibella EV, Adluru G, Hsu EW. Model-based reconstruction of undersampled diffusion tensor k-space data. Magn Reson Med 2013;70:429-440
15. Tran-Gia J, Stab D, Wech T, Hahn D, Kostler H. Model-based acceleration of parameter mapping (MAP) for saturation prepared radially acquired data. Magn Reson Med 2013;70:1524-1534
16. Zhu Y, Peng X, Wu Y, et al. Direct diffusion tensor estimation using a model-based method with spatial and parametric constraints. Med Phys 2017;44:570-580
17. Peng X, Ying L, Liu Y, Yuan J, Liu X, Liang D. Accelerated exponential parameterization of T2 relaxation with model-driven low rank and sparsity priors (MORASA). Magn Reson Med 2016;76:1865-1878
18. Chu ML, Chang HC, Oshio K, Chen NK. A single-shot T2 mapping protocol based on echo-split gradient-spin-echo acquisition and parametric multiplexed sensitivity encoding based on projection onto convex sets reconstruction. Magn Reson Med 2018;79:383-393
19. Zhu Y, Liu Y, Ying L, et al. SCOPE: signal compensation for low-rank plus sparse matrix decomposition for fast parameter mapping. Phys Med Biol 2018;63:185009
20. Zhu B, Liu JZ, Cauley SF, Rosen BR, Rosen MS. Image reconstruction by domain-transform manifold learning. Nature 2018;555:487-492
21. Quan TM, Nguyen-Duc T, Jeong WK. Compressed sensing MRI reconstruction using a generative adversarial network with a cyclic loss. IEEE Trans Med Imaging 2018;37:1488-1497
22. Mardani M, Gong E, Cheng JY, et al. Deep generative adversarial neural networks for compressive sensing MRI. IEEE Trans Med Imaging 2019;38:167-179
23. Han Y, Yoo J, Kim HH, Shin HJ, Sung K, Ye JC. Deep learning with domain adaptation for accelerated projection-reconstruction MR. Magn Reson Med 2018;80:1189-1205
24. Lee D, Yoo J, Tak S, Ye JC. Deep residual learning for accelerated MRI using magnitude and phase networks. IEEE Trans Biomed Eng 2018;65:1985-1995
25. Wang S, Ke Z, Cheng H, et al. DIMENSION: dynamic MR imaging with both k-space and spatial prior knowledge obtained via multi-supervised network training. NMR Biomed 2019:e4131
26. Eo T, Jun Y, Kim T, Jang J, Lee HJ, Hwang D. KIKI-net: cross-domain convolutional neural networks for reconstructing undersampled magnetic resonance images. Magn Reson Med 2018;80:2188-2201
27. Yang Y, Sun J, Li H, Xu Z. ADMM-CSNet: a deep learning approach for image compressive sensing. IEEE Trans Pattern Anal Mach Intell 2020;42:521-538

28. Hammernik K, Klatzer T, Kobler E, et al. Learning a variational network for reconstruction of accelerated MRI data. Magn Reson Med 2018;79:3055-3071
29. Aggarwal HK, Mani MP, Jacob M. MoDL: model-based deep learning architecture for inverse problems. IEEE Trans Med Imaging 2019;38:394-405
30. Schlemper J, Caballero J, Hajnal JV, Price AN, Rueckert D. A deep cascade of convolutional neural networks for dynamic MR image reconstruction. IEEE Trans Med Imaging 2018;37:491-503
31. Adler J, Oktem O. Learned primal-dual reconstruction. IEEE Trans Med Imaging 2018;37:1322-1332
32. Qin C, Schlemper J, Caballero J, Price AN, Hajnal JV, Rueckert D. Convolutional recurrent neural networks for dynamic MR image reconstruction. IEEE Trans Med Imaging 2019;38:280-290
33. Cai C, Wang C, Zeng Y, et al. Single-shot T2 mapping using overlapping-echo detachment planar imaging and a deep convolutional neural network. Magn Reson Med 2018;80:2202-2214
34. Liu F, Feng L, Kijowski R. MANTIS: Model-Augmented Neural neTwork with Incoherent k-space Sampling for efficient MR parameter mapping. Magn Reson Med 2019;82:174-188
35. Cohen O, Zhu B, Rosen MS. MR fingerprinting Deep RecOnstruction NEtwork (DRONE). Magn Reson Med 2018;80:885-894
36. Yang J, Zhang Y, Yin W. A fast alternating direction method for TVL1-L2 signal reconstruction from partial Fourier data. IEEE J Sel Top Signal Process 2010;4:288-297
37. Lingala SG, Hu Y, DiBella E, Jacob M. Accelerated dynamic MRI exploiting sparsity and low-rank structure: k-t SLR. IEEE Trans Med Imaging 2011;30:1042-1054
38. Cheng J, Ke Z, Wang H, et al. Learning reconstruction without ground-truth data: an unsupervised way for fast MR imaging. In Proceedings of the 28th Annual Meeting of ISMRM, 2020:3634
39. Lustig M, Donoho D, Pauly JM. Sparse MRI: the application of compressed sensing for rapid MR imaging. Magn Reson Med 2007;58:1182-1195
40. Lustig M, Donoho DL, Santos JM, Pauly JM. Compressed sensing MRI. IEEE Signal Process Mag 2008;25:72-82
41. Liang D, Liu B, Wang J, Ying L. Accelerating SENSE using compressed sensing. Magn Reson Med 2009;62:1574-1584
42. Liang D, Cheng J, Ke Z, Ying L. Deep magnetic resonance image reconstruction: inverse problems meet neural networks. IEEE Signal Process Mag 2020;37:141-151
43. Cheng J, Wang H, Ying L. Model learning: primal dual networks for fast MR imaging. Medical Image Computing and Computer Assisted Intervention - MICCAI 2019, 22nd International Conference, Shenzhen, China, 2019:21-29
44. Walsh DO, Gmitro AF, Marcellin MW. Adaptive reconstruction of phased array MR imagery. Magn Reson Med 2000;43:682-690
45. Baboli R, Sharafi A, Chang G, Regatte RR. Isotropic morphometry and multicomponent T1 rho mapping of human knee articular cartilage in vivo at 3T. J Magn Reson Imaging 2018;48:1707-1716
46. Sharafi A, Xia D, Chang G, Regatte RR. Biexponential T1rho relaxation mapping of human knee cartilage in vivo at 3 T. NMR Biomed 2017;30
47. Zhu Y, Liu Y, Ying L, Liu X, Zheng H, Liang D. Bio-SCOPE: fast biexponential T1rho mapping of the brain using signal-compensated low-rank plus sparse matrix decomposition. Magn Reson Med 2020;83:2092-2106